Improvised Absorbing Boundary Conditions for Three-dimensional Electromagnetic Finite Elements

K. Sugahara[1]

Abstract – **Improvised absorbing boundary conditions for high frequency electromagnetic problems have been studied. This method approximated unbounded space as series of isotropic spherical shells so as to emulate open boundaries without the need for additional code to any finite element solver. Previous work addressed applications of this technique to magnetostatic and electrostatic problems. This present work studies the wide-range frequency dependence of the IABC when applied to three-dimensional electromagnetic radiation problems.**

1 INTRODUCTION

Although open boundary techniques for electromagnetic finite elements are an old research topic and lots of work has been done so far [1]-[12], it is still discussed in the recent literature [13]-[17]. Recently, Improvised Asymptotic Boundary condition (IABC) was proposed [16, 17]. This method approximated unbounded space as series of isotropic shells so as to emulate open boundaries. Those isotropic shells work on the same principle as other realizations of asymptotic boundary conditions, by reproducing the impedance of an unbounded region for low-order harmonics. The negligible error is introduced by not exactly modeling the boundary impedance for higher order harmonics. First-order ABCs specify the parameters of a mixed-type boundary condition that match the far-field characteristics of a magnetic dipole. While higher order ABCs that emulate the far-field behavior of multipoles are possible and provide improved accuracy. The biggest advantage of this method is that it requires no additional code to any finite element solver [16, 17]. In this paper, we extend the method to three-dimensional high-frequency electromagnetic wave propagation problems. The first-order Improvised Absorbing Boundary Conditions (hereafter IABC) in three-dimensional wave propagation finite element problems are presented. We have employed a commercial finite element solver FEMTET@ [18, 19] and studied the first-order IABC form static to high frequencies.

2 FORMULATION

Three-dimensional electromagnetic fields can be expressed with the sum of magnetic and electrical vector potentials; A_r, and F_r [20]. The derivatives of the two potentials give the electromagnetic fields as (1). The vector potentials; A_r, and F_r divided by r obey the Helmholz equations (2), where k_0 is the wavenumber of the vacuum, $\tilde{\varepsilon}$ and $\tilde{\mu}$ is the relative permeability and relative permittivity, respectively.

$$\begin{cases} E_r = \dfrac{1}{j\omega\tilde{\varepsilon}}\left[\dfrac{\partial^2}{\partial r^2}+k^2\right]A_r = \dfrac{1}{j\omega\tilde{\varepsilon}}\left[\dfrac{-1}{r^2\sin\theta}\dfrac{\partial}{\partial\theta}(\sin\theta\dfrac{\partial}{\partial\theta})+\dfrac{-1}{r^2\sin\theta}\dfrac{\partial^2}{\partial\phi^2}\right]A_r \\ E_\theta = \dfrac{-1}{r\sin\theta}\dfrac{\partial F_r}{\partial\phi}+\dfrac{1}{j\omega\tilde{\varepsilon}}\dfrac{1}{r}\dfrac{\partial^2 A_r}{\partial r\partial\theta} \\ E_\phi = \dfrac{1}{r}\dfrac{\partial F_r}{\partial\theta}+\dfrac{1}{j\omega\tilde{\varepsilon}}\dfrac{1}{r\sin\theta}\dfrac{\partial^2 A_r}{\partial r\partial\phi} \end{cases}$$

$$\begin{cases} H_r = \dfrac{1}{j\omega\tilde{\mu}}\left[\dfrac{\partial^2}{\partial r^2}+k^2\right]F_r = \dfrac{1}{j\omega\tilde{\mu}}\left[\dfrac{-1}{r^2\sin\theta}\dfrac{\partial}{\partial\theta}(\sin\theta\dfrac{\partial}{\partial\theta})+\dfrac{-1}{r^2\sin\theta}\dfrac{\partial^2}{\partial\phi^2}\right]F_r \\ H_\theta = \dfrac{1}{r\sin\theta}\dfrac{\partial A_r}{\partial\phi}+\dfrac{1}{j\omega\tilde{\mu}}\dfrac{1}{r}\dfrac{\partial^2 F_r}{\partial r\partial\theta} \\ H_\phi = -\dfrac{1}{r}\dfrac{\partial A_r}{\partial\theta}+\dfrac{1}{j\omega\tilde{\mu}}\dfrac{1}{r\sin\theta}\dfrac{\partial^2 F_r}{\partial r\partial\phi} \end{cases} \tag{1}$$

$$\begin{cases} \left(\Delta+k^2\right)\dfrac{A_r}{r}=0 \\ \left(\Delta+k^2\right)\dfrac{F_r}{r}=0 \end{cases} \tag{2}$$

The solutions of the Helmholz equations are expanded with (4). $h_n^{(1)}(kr)$ corresponds to the incoming wave and $h_n^{(2)}(kr)$ outgoing wave, therefore, open boundary solutions can be expressed in the form of (4). and open boundary solutions are expressed in the form of (5).

$$\begin{cases} \dfrac{A_r}{r}=\sum_{n,m} a_n^m h_n^{(2)}(kr)Y_n^m(\theta,\phi)+b_n^m h_n^{(1)}(kr)Y_n^m(\theta,\phi) \\ \dfrac{F_r}{r}=\sum_{n,m} f_n^m h_n^{(2)}(kr)Y_n^m(\theta,\phi)+g_n^m h_n^{(1)}(kr)Y_n^m(\theta,\phi) \end{cases} \tag{3}$$

$$\begin{cases} \dfrac{A_r}{r}=\sum_{n,m} a_n^m h_n^{(2)}(kr)Y_n^m(\theta,\phi) \\ \dfrac{F_r}{r}=\sum_{n,m} f_n^m h_n^{(2)}(kr)Y_n^m(\theta,\phi) \end{cases} \tag{4}$$

$$k=\sqrt{\tilde{\varepsilon}\tilde{\mu}}k_0$$

whereas k is a wave number in each shell and k_0 is a wave number of vacuum.

Figure 1 shows a schematic image of the first-order improvised absorbing condition. The region of interest is inside the inner boundary and the outer shells work as absorbers. The exterior boundary is a PEC.

[1] Department of Electric and Electronic Engineering, 3-4-1, Kowakae, Higashi-Osaka, Osaka, 577-8502, Japan,
e-mail: ksugahar@kindai.ac.jp, tel.: +81643073496

978-1-4799-7806-9/15/$31.00 ©2015 IEEE

The continuity conditions (5) must hold at each boundary of the adjacent two shells, and they can be expressed as eq. (6) with vector potentials, A_r, and F_r. At the exterior boundary, the boundary condition is given as (7) which gives (8) in the spectrum domain.

$$\begin{cases} D_r^{n+1} = D_r^n \\ E_\theta^{n+1} = E_\theta^n \\ E_\phi^{n+1} = E_\phi^n \end{cases} \quad \begin{cases} B_r^{n+1} = B_r^n \\ H_\theta^{n+1} = H_\theta^n \\ H_\phi^{n+1} = H_\phi^n \end{cases} \tag{5}$$

$$\begin{cases} A_r^{n+1} = A_r^n \\ \tilde{\varepsilon}^{n+1} \dfrac{\partial A_r^{n+1}}{\partial r} = \tilde{\varepsilon}^{n} \dfrac{\partial A_r^{n+1}}{\partial r} \end{cases} \quad \begin{cases} F_r^{n+1} = F_r^n \\ \tilde{\mu}^{n+1} \dfrac{\partial F_r^{n+1}}{\partial r} = \tilde{\mu}^{n} \dfrac{\partial F_r^{n+1}}{\partial r} \end{cases} \tag{6}$$

$$\begin{cases} E_\theta = 0 \\ B_r = 0 \end{cases} \tag{7}$$

$$\begin{cases} a_N \varsigma_n'^{(2)}(k_N r_{N+1}) + b_N \varsigma_n'^{(1)}(k_N r_{N+1}) = 0 \\ f_N \dfrac{1}{\tilde{\mu}_N} \varsigma_n^{(2)}(k_N r_{N+1}) + g_N \dfrac{1}{\tilde{\mu}_N} \varsigma_n^{(1)}(k_N r_{N+1}) = 0 \end{cases} \tag{8}$$

whereas $\varsigma_n^{(1)}(kr)$ are defined by $\begin{cases} \varsigma_n^{(1)}(kr) = r h_n^{(1)}(kr) \\ \varsigma_n^{(2)}(kr) = r h_n^{(2)}(kr) \end{cases}$

We define two matrices defined by (9) which are dependent on relative complex permeability $\tilde{\varepsilon}_i$ and relative complex rermittivity $\tilde{\mu}_i$ of each shell.

$$\boldsymbol{E}_j^{(n)}(\tilde{\varepsilon}_i, \tilde{\mu}_i) = \begin{bmatrix} \dfrac{1}{\tilde{\varepsilon}_i} \varsigma_n^{(2)}(k_i r_j) & \dfrac{1}{\tilde{\varepsilon}_k} \varsigma_n^{(1)}(k_i r_j) \\ \varsigma_n'^{(2)}(k_i r_j) & \varsigma_n'^{(1)}(k_i r_j) \end{bmatrix}$$

$$\boldsymbol{U}_j^{(n)}(\tilde{\varepsilon}_i, \tilde{\mu}_i) = \begin{bmatrix} \dfrac{1}{\tilde{\mu}_i} \varsigma_n^{(2)}(k_i r_j) & \dfrac{1}{\tilde{\mu}_k} \varsigma_n^{(1)}(k_i r_j) \\ \varsigma_n'^{(2)}(k_i r_j) & \varsigma_n'^{(1)}(k_i r_j) \end{bmatrix} \tag{9}$$

From (6) and (8), (10) is obtained which is the formula for the IABC. Once $\tilde{\varepsilon}_i$ and $\tilde{\mu}_i$ are obtained by solving (10), the IABC will give the approximate open boundary solution up to the same order as the number of layers.

$$\begin{cases} 0 = \begin{bmatrix} 0 & 1 \end{bmatrix} \boldsymbol{E}_N^{(n)}(\tilde{\varepsilon}_N, \tilde{\mu}_N) \boldsymbol{E}_N^{(n)}(\tilde{\varepsilon}_{N-1}, \tilde{\mu}_{N-1})^{-1} \cdots \\ \quad \cdots \boldsymbol{E}_1^{(n)}(\tilde{\varepsilon}_1, \tilde{\mu}_1) \boldsymbol{E}_0^{(n)}(\tilde{\varepsilon}_1, \tilde{\mu}_1)^{-1} \boldsymbol{E}_0^{(n)}(\tilde{\varepsilon}_0, \tilde{\mu}_0) \begin{bmatrix} 1 \\ 0 \end{bmatrix} \\ 0 = \begin{bmatrix} 1 & 0 \end{bmatrix} \boldsymbol{U}_N^{(n)}(\tilde{\varepsilon}_N, \tilde{\mu}_N)^{-1} \boldsymbol{U}_N^{(n)}(\tilde{\varepsilon}_{N-1}, \tilde{\mu}_{N-1}) \cdots \\ \quad \cdots \boldsymbol{U}_1^{(n)}(\tilde{\varepsilon}_1, \tilde{\mu}_1) \boldsymbol{U}_0^{(n)}(\tilde{\varepsilon}_1, \tilde{\mu}_1)^{-1} \boldsymbol{U}_0^{(n)}(\tilde{\varepsilon}_0, \tilde{\mu}_0) \begin{bmatrix} 1 \\ 0 \end{bmatrix} \end{cases} \tag{10}$$

In this paper, we focus on the first-order IABC formulated by (11).

$$\begin{cases} 0 = \begin{bmatrix} 0 & 1 \end{bmatrix} \boldsymbol{E}_1^{(1)}(\tilde{\varepsilon}_1, \tilde{\mu}_1) \boldsymbol{E}_0^{(1)}(\tilde{\varepsilon}_1, \tilde{\mu}_1)^{-1} \boldsymbol{E}_0^{(1)}(\tilde{\varepsilon}_0, \tilde{\mu}_0) \begin{bmatrix} 1 \\ 0 \end{bmatrix} \\ 0 = \begin{bmatrix} 1 & 0 \end{bmatrix} \boldsymbol{U}_1^{(1)}(\tilde{\varepsilon}_1, \tilde{\mu}_1) \boldsymbol{U}_0^{(1)}(\tilde{\varepsilon}_1, \tilde{\mu}_1)^{-1} \boldsymbol{U}_0^{(1)}(\tilde{\varepsilon}_0, \tilde{\mu}_0) \begin{bmatrix} 1 \\ 0 \end{bmatrix} \end{cases} \tag{11}$$

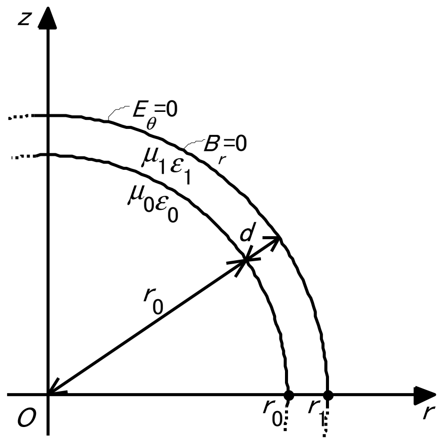

Figure 1: Schematic image of the first-order improvised absorbing condition. The region of interest is inside the inner boundary and the outer shell works as an absorber. The exterior boundary is a PEC.

3 SOLUTION OF NONLINEAR EQUATION

The numerical solutions of the non-linear equations (11) are obtained with the quasi-Newton method which is sensitive to the values of initial approximation. In order to obtain solutions which smoothly connect to the magnetostatic and electrostatic solutions, the following optimization procedure is performed. Starting from the lowest frequency, the static solutions, discussed in [16, 17], are chosen to be initial values of the quasi-Newton method. Those values have real part only. Then the frequency is incremented by Δf using the previously obtained result as an initial value. The incrimination of the frequency was repeated until the highest frequency using the former results as initial values. By doing so, the solutions smoothly connected to the static solutions, as shown in Figure 3 and Table I, are obtained. Otherwise (11) do not have a unique solution but multiple solutions.

TABLE I
COMPLEX RELATIVE PERMEABILITY AND PERMITTIVITY OF IABC

ω / c	μ	ε
0.06	10.099-0.002j	0.181-0.000j
2.00	0.800-6.104j	0.094+0.157j
6.00	0.039-1.533j	0.111+0.592j
20.00	0.004-0.092j	0.310+5.682j

4 NUMERICAL EXAMPLES

In order to verify the previous discussion, we have employed a commercial finite element solver FEMTET@ to solve wave radiation from an electrically small dipole shown in Figure 2. We compared the obtained results with the analytical solution of the electrically small dipole (12) as shown Figure 2. E_r and E_θ are plotted along the white horizontal and vertical lines, respectively Exact matches inside the first-order IABC were observed.

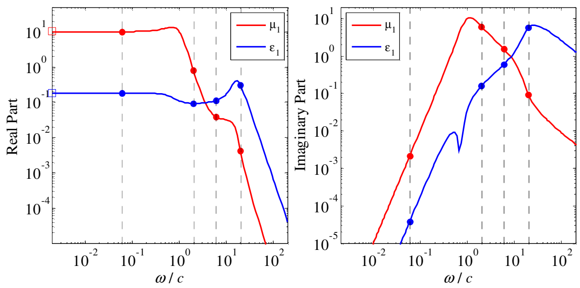

Figure 3: Normalized angular frequency dependence of the relative permeability and the relative permittivity of the first-order IABC

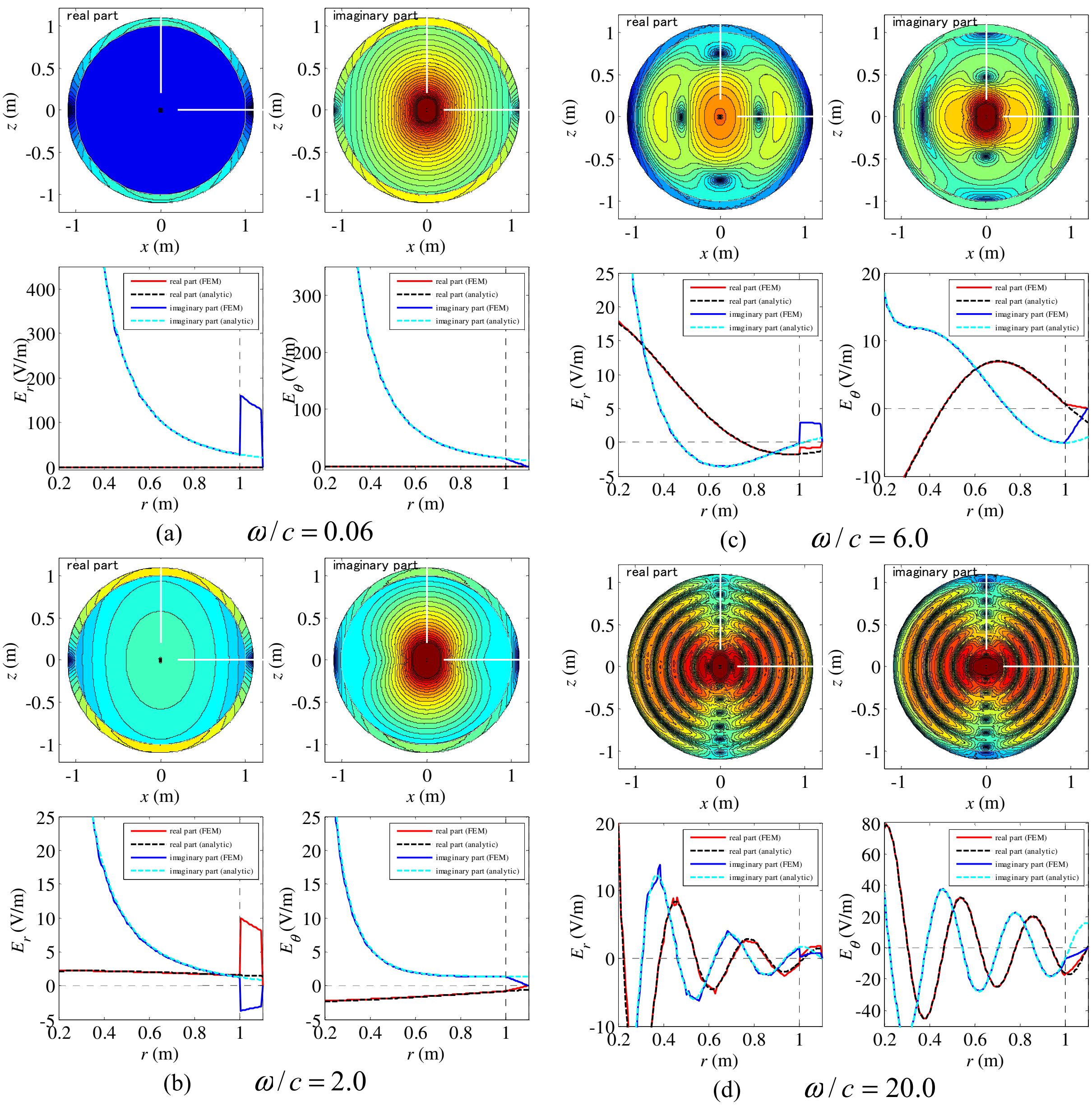

Figure 2: Contour plots and electric field along white lines compared with the analytical solutions.

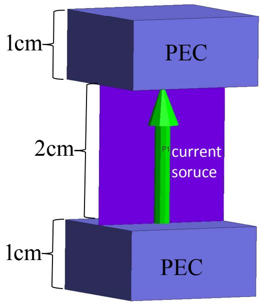

Fig. 4. Electrically small dipole modelled in the FEM analysis.

$$\begin{cases} E_r = \dfrac{Idl}{2\pi}\eta(k^2e^{-jkr})\left[\dfrac{1}{(kr)^2} - j\dfrac{1}{(kr)^3}\right]\cos\theta \\ E_\theta = \dfrac{Idl}{4\pi}\eta(k^2e^{-jkr})\left[j\dfrac{1}{kr} + \dfrac{1}{(kr)^2} - j\dfrac{1}{(kr)^3}\right]\sin\theta \\ H_\phi = \dfrac{Idl}{4\pi}(k^2e^{-jkr})\left[j\dfrac{1}{kr} + \dfrac{1}{(kr)^2}\right]\sin\theta \end{cases} \quad (12)$$

5 CONCLUSION

We have studied the first-order IABC with the electrically small dipole. The IABC is seamlessly appreciable to both static and high frequency problems.

Acknowledgments

The author would like to thank Dr. David Meeker for his valuable comments on this study. The author also would like to thank Prof. Akira Komiyama for his valuable discussions this study.

References

[1] J. Jin, *The Finite Element Method in Electromagnetics*, John Wiley & Sons, Inc. New York 1993.
[2] A. B. J. Reece and T. W. Preston, *Finite Element Methods in Electrical Power Engineering*, Oxford University Press, New York, 2000
[3] J. L. Volakis, A. Chatterjee, and L.-C. Kempel, *Finite Element Method for Electromagnetics*. New York: IEEE, 1998.
[4] Q. Chen and A. Konrad, “A review of finite element open boundary techniques for static and quasi-static electromagnetic field problems,” *IEEE Trans. Magn.*, vol. 33, pp. 663–676, Jan. 1997.
[5] P. Bettess, “Infinite elements,” *Int. J. Num. Meth Engng*., vol. 11, pp.53–64, 1977.
[6] E. M. Freeman and D. A. Lowther, “A novel mapping technique for open boundary finite element solutions to Poisson’s equation,” *IEEE Trans. Magn*., vol. 24, no. 6, pp. 2934–2936, Nov. 1988.
[7] S. Gratkowski et al., “Asymptotic boundary conditions for the finite element modeling of axisymmetric electrical field problems,” *IEEE Trans. Magn*., vol. 36, pp. 717-721, July 2000.
[8] T. G. Moore, J. G. Blaschak, A. Taflove, and G. A. Krigsmann, “Theory and application of radiation boundary operators.” *IEEE Trans. Antennas Propaget*., vol. AP-36, p.1797-1812, Dec. 1988.
[9] A. F. Peterson, “Accuracy of 3-D radiation boundary conditions for use with the vector Helmholtz equation,” *IEEE Trans. Antennas Propagat*., vol. 40, pp. 351–355, Mar. 1992.
[10] J. P. Berenger, “A perfect matched layer for the absorption of electromagnetic waves”, J. Comp. Phys., Vol. 114, pp. 185-200, 1994.
[11] J. Fang and Z. Wu, “Generalized perfect matched layer for the absorption of propagating and evanescent waves in lossless and lossy media,” *IEEE Runs. Microwave Theory Tech*., vol. 14, pp. 2216-2222, 1996.
[12] J. M. Jin, J. L. Volakis, and V. V. Liepa, “An engineer's approach for terminating finite element meshes in scattering analysis,” *1991 IEEE AP-S Symposium Digest*, vol. 2, pp. 1216-1219, June 1991.
[13] K. Sugahara, “Generalized electrical image method for field reconstruction,” *IEEE Trans. Appl. Supercond*., vol. 22, no. 4, p. 4004507, Aug. 2012.
[14] K. Sugahara, “Generalized strategic dual image method for open boundary axisymmetrical magnetic field problems,” *IEEE Trans. Magn*., vol. 49, no. 4, p. 4944-4950, Sept. 2013.
[15] K. Sugahara, “Periodic image method for open boundary axisymmetical magnetic field problems,” *IEEE Trans. Magn*., vol. 49, no. 11, p. 5399-5403, Nov. 2013.
[16] D. Meeker, “Improvised open boundary conditions for magnetic finite elements,” *IEEE Trans. Magn*., vol. 49, pp. 5243-5247, Oct. 2013.
[17] D. Meeker, “Improvised asymptotic boundary conditions for electrostatic finite elements,” *IEEE Trans. Magn*., vol. 50, no. 6, pp. 7400609, June. 2014.
[18] Hosotani, Tatsuya, and Ikuo Awai. "A novel analysis of ZVS wireless power transfer system using coupled resonators." *Microwave Workshop Series on Innovative Wireless Power Transmission: Technologies, Systems, and Applications (IMWS), 2012 IEEE MTT-S International*. IEEE, 2012. P. 235-238
[19] http://www.muratasoftware.com.
[20] R. F. Harrington, *Time-Harmonic Electromagnetic Fields*. New York: McGrwa-Hill, 1961.: